RESEARCH ARTICLE • OPEN ACCESS

Dynamical Analysis of a Crowley–Martin Eco-Epidemiological Model with Impact of Fear, Prey Refuge, and Harvesting

Arumugam Divya *et al.*

Volume 6, Issue 4, Pages 363–375, December 2025

Received 22 September 2025, Revised 18 November 2025, Accepted 26 November 2025, Published Online 24 December 2025

To Cite this Article : A. Divya *et al.*,"Dynamical Analysis of a Crowley–Martin Eco-Epidemiological Model with Impact of Fear, Prey Refuge, and Harvesting", *Jambura J. Biomath*, vol. 6, no. 4, pp. 363–375, 2025, *https://doi.org/10.37905/jjbm.v6i4.34528*

JOURNAL INFO • JAMBURA JOURNAL OF BIOMATHEMATICS

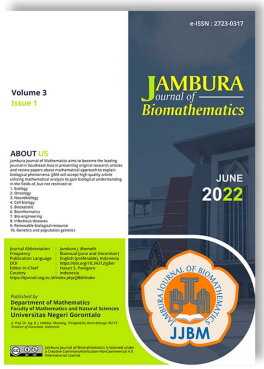

Homepage	:	http://ejurnal.ung.ac.id/index.php/JJBM/index
Journal Abbreviation	:	Jambura J. Biomath.
Frequency	:	Quarterly (March, June, September and December)
Publication Language	:	English
DOI	:	https://doi.org/10.37905/jjbm
Online ISSN	:	2723-0317
Editor-in-Chief	:	Hasan S. Panigoro
Publisher	:	Department of Mathematics, Universitas Negeri Gorontalo
Country	:	Indonesia
OAI Address	:	http://ejurnal.ung.ac.id/index.php/jjbm/oai
Google Scholar ID	:	XzYgeKQAAAAJ
Email	:	editorial.jjbm@ung.ac.id

JAMBURA JOURNAL • FIND OUR OTHER JOURNALS

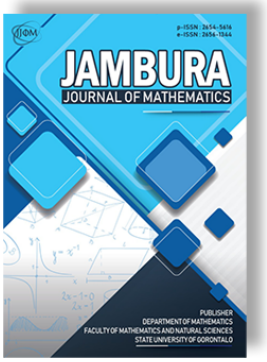

Jambura Journal of Mathematics

Jambura Journal of Mathematics Education

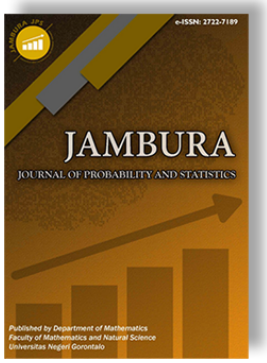

Jambura Journal of Probability and Statistics

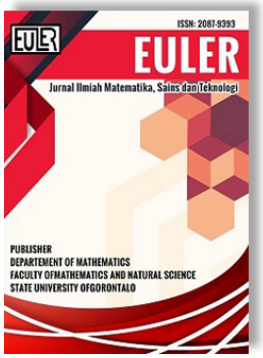

EULER : Jurnal Ilmiah Matematika, Sains, dan Teknologi

Jambura Journal of Biomathematics, Volume 6, Issue 4, Pages 363–375, December 2025 https://doi.org/10.37905/jjbm.v6i4.34528

Research Article

Check for updates

Dynamical Analysis of a Crowley–Martin Eco-Epidemiological Model with Impact of Fear, Prey Refuge, and Harvesting

Arumugam Divya[1], **Muthurathinam Sivabalan**[2,*], **Mehmet Yavuz**[3,4,*], **Anbulinga Ashwin**[2], **and Manickasundaram Siva Pradeep**[5]

[1]*Department of Mathematics, INFO Institute of Engineering, Coimbatore, Tamilnadu, India*
[2]*Department of Mathematics, Sri Ramakrishna Mission Vidyalaya College of Arts and Science, Coimbatore, Tamilnadu, India*
[3]*Department of Mathematics and Computer Sciences, Necmettin Erbakan University, Konya, Turkiye*
[4]*Department of Applied Mathematics and Informatics, Kyrgyz-Turkish Manas University, Bishkek 720038, Kyrgyzstan*
[5]*Department of Mathematics, United Institute of Technology, Coimbatore, Tamilnadu, India*

ARTICLE HISTORY
Received 22 September 2025
Revised 18 November 2025
Accepted 26 November 2025
Published 24 December 2025

KEYWORDS
Fear effect
Refuge
Harvesting
Stability analysis
Hopf-bifurcation

ABSTRACT. *We develop an eco-epidemiological model that includes three species comprising a food web: vulnerable prey, diseased prey, and predator species that transmit disease to their prey. A population of prey consists of two subpopulations: healthy prey (susceptible prey), which follow the logistic law and are capable of reproducing, and diseased prey, which are destroyed by predation or die before reproducing. A predator devour vulnerable and infected prey in various proportions in a Crowley-Martin type of interaction. In the Crowley-Martin functional response, there is interdependence among predators, regardless of whether a particular predator is actively seeking prey or interacting with prey at any given time. In Holling-type II interactions, vulnerable prey is consumed by infected prey.*

1. Introduction

Ecology is a branch of study that deals with living organisms and their surroundings. Epidemiology is the scientific investigation of the prevalence, events, and determinants (risk factors, causes) of health-related conditions and occurrences in particular populations (state, country, global). Integrating ecology and epidemiology, eco-epidemiology is a rapidly growing field in mathematical biology. These two branches exist in the literature and have been explored separately. The basis for the development of model dynamics through many mathematical models was established by the early discoveries of Lotka [25] and Volterra [52]. It has been studied quantitatively using multiple equation constructs ranging from standard models governed by ordinary, partial and random differential equations with respect to various objectives in the environmental domain. These mathematical models are intensively analyzed to explore various environmental effects, stating from their interactions [19], hunting cooperation [2], supplementary food source [29], Allee effect [12], prey refuge [42], fear effect [53] to harvesting [18]. Kermack and McKendrick [23] were pioneers in the study of the quantitative transmission of diseases. Several investigations have been conducted independently in both fields. However, in the latter part of the 1990s, these two crucial fields of research began to overlap, and eco-epidemiology emerged as a new field of study. The field of eco-epidemiology was introduced by Anderson and May [3] on the premise that disease presence affects how a predator and diseased prey interact. According to [5, 24], the predator-prey model system has been one of the most significant subjects in biological systems. The predator-prey interactions play a vital role in determining the stability and persistence of many species in ecosystems [1]. Organisms' survival depends on how efficiently they eat or take their food resources (such as prey for predators, while prey serves as food resources and energy for associated predators). Consequently, the specific predator directly affects the prey population as well as the interconnected ecosystem. Numerous functional reactions have been used to quantitatively depict these direct interactions between predator and prey. A key component of predator-prey interactions is the functional response [5]. Gaining further biological understanding into predator-prey interactions can be facilitated by comprehending the purpose of reactions. The Crowley–Martin functional response [13] is advantageous because it incorporates predator interference during both searching and handling phases, making it biologically more realistic than Holling Type II and Beddington–DeAngelis models. By reducing predation efficiency when predator density is high, it avoids overestimating consumption and better reflects natural crowding effects. As a result, it produces more accurate and ecologically meaningful predator–prey dynamics [16, 48, 50]. There is very little literature on the predator-prey model with the Crowley-Martin functional response [51]. The Crowley–Martin functional response is predator dependent. The per capita feeding rate for predator P in this formulation is

$$f(S,P) = \frac{\beta S}{(1+\eta S)(1+\mu P)},$$

*Corresponding Author.

Email : *sivabalan8890@gmail.com, mehmetyavuz@erbakan.edu.tr* (M. Sivabalan, Mehmet Yavuz)
Homepage : http://ejurnal.ung.ac.id/index.php/JJBM/index / E-ISSN : 2723-0317

where β, η, μ are positive factors utilized in the feeding rate that correspond to the handling time, catch rate, and amount of predator interference, respectively. Nasir et al. [38] found that delay parameters significantly influence the stability of the diabetic population model, with certain delays causing a switch from stability to instability and leading to periodic dynamics. Additionally, reducing the rates of diabetes development and improving medical resource allocation can notably decrease diabetes cases and complications.

A predator-prey model of the Lotka-Volterra type with a Michaelis-Menten-type functional response is examined in this study. According to Holling [20], each predator's functional reaction approaches a constant as the quantity of prey increases, indicating that the prey population density in this model is resource-limited. A spatial refuge also protects a portion of the prey from predators. In reality, not all prey are felled by predators, as they often have safe havens that can be avoided [21, 45]. The study of predator–prey models that incorporate prey refuge is a prominent topic in biomathematics, and numerous studies have advanced our understanding of such systems [26–28, 34, 43]. Several researchers [7, 8, 22, 31, 39, 44, 46] have employed deterministic and fractional models in disease dynamics to investigate stability and bifurcation.

Most of the time, diseased species are the main source of disease spreading among non-infected species. Removal of contaminated populations (eradication) is therefore one of the most frequently used and important strategies to prevent disease transmission [4, 49]. The exploitation of environmental resources and harvesting of population species are commonly practiced in fisheries, forestry, agriculture, biocontrol programs, and wildlife management. Various studies reveal the different impacts of harvesting on the system. In research, harvesting is occasionally seen as a moderating factor. Further, the inappropriate amount of imposed harvesting schemes may be the cause of the extinction of the species. Many authors have shown interest in analyzing the harvested prey-predator model [4, 6, 9, 11, 14, 30]. Parasites may reduce both biomass and yield by increasing mortality, reducing fertility, and affecting or reducing the population size structure of harvested stocks [15].

Several recent studies have contributed significantly to the development of nonlinear dynamical analysis, iterative numerical methods, and fractional-order modelling [10, 35–37, 40, 41]. These works highlight the increasing use of advanced numerical techniques and fractional calculus for improving stability, convergence, and dynamic interpretation in complex biological and ecological systems. Many studies ignore the effects of fear, refuge, and harvest in favor of focusing exclusively on the dynamics of predator-prey interactions within the framework of Crowley-Martin's ecological-epidemiological paradigm. There are very few studies in the literature that look at prey-predator models that involve interactions between two species, such as Crowley-Martin disease, in prey populations without fear effect. As far as we are aware, a lack of research has been done on the Crowley-Martin eco-epidemiological model that incorporates the level of fear, refuge and harvesting. Inspired by this fact, we explore the level of fear on the diseased prey-predator model and susceptible prey populations through Crowley-Martin-type interactions. The current focus is on investigating and analyzing the impact of fear, prey refuge, and harvesting the predator-prey paradigm. A comprehensive study is conducted on the dynamical characteristics of the current model system, which include transcritical, saddle-node, and Hopf bifurcation propagation. This study takes into account an eco-epidemiological setting, including harvesting and refuge from predators, as well as the impact of fear. This proposed model differs from earlier works in that it uses Crowley-Martin-type interactions. An explanation of the structure of this work is provided below. Section 2 provides a detailed description of the proposed model. Section 3 discusses the positivity and boundedness of the proposed system. In Section 4, the stability analysis of every equilibrium point is described along with its existence. Bifurcation analyses for harvesting are explained in Section 5. Section 6 examines quantitative results for the suggested model in support of the qualitative findings.

2. Mathematical model formation

Basically, there are two sorts of populations in the model: (i), which is the prey population with density $N(t)$, and (ii), which is the predator population with concentration $P(t)$. The following presumptions have been considered for developing the model:

- There are some infectious diseases in the prey population and predators encounter both healthy and infected prey. As a result of the illness, the prey population is assumed to be split into two sub-classes: the vulnerable prey $S(T)$ and the diseased prey $I(T)$, i.e., at any time $T, N(T) = S(T) + I(T)$. R is the vulnerable prey's intrinsic growth rate.
- When there is no disease, a logistic equation with carrying capacity $K(K > 0)$ states that the prey population density rises.
- Also, the sick prey encounters the vulnerable prey through a type II Holling functional response as $\frac{\alpha_1 SI}{a_1+S}$, where α_1 denotes the infection rate at which susceptible prey acquire infection from infected prey. Here, a_1 represents the half-saturation constants, and α_1 represents the infection rate for susceptible prey. Table 1 shows the descriptions of the parameters.
- The predator population uses a functional response akin to Crowley-Martin's to devour the prey population. Here, the prey are vulnerable to the rate of consumption, rate of capture, handling time, and amount of interference among the predator populations on feeding rate, respectively, for β_1, b_1, η_1, and μ_1.
- For vulnerable and diseased prey, the adaptation efficiency of predators is defined as $c, (0 < c < 1)$, respectively. Additionally, D_1 represents the diseased prey mortality rate, and D_2 represents the natural predator mortality rate.

$$\begin{aligned}
\frac{dS}{dT} &= \left(1 - \frac{S+I}{K}\right) RS - \frac{\alpha_1 S I}{a_1 + S} - \frac{\beta_1 S P}{(1+\eta_1 S)(1+\mu_1 P)},\\
\frac{dI}{dT} &= \frac{\alpha_1 S I}{a_1 + S} - D_1 I - \frac{b_1 I P}{(1+\eta_1 I)(1+\mu_1 P)},\\
\frac{dP}{dT} &= -D_2 P + \frac{c\, b_1 I P}{(1+\eta_1 I)(1+\mu_1 P)} + \frac{c\, \beta_1 S P}{(1+\eta_1 S)(1+\mu_1 P)}.
\end{aligned} \tag{1}$$

Initially, we incorporate the fear effect into the model (1). The influence of fear, sometimes referred to as predator avoidance

Table 1. Model Variables and Parameters with Biological Meaning and Units

Symbol	Meaning	Units
S	Density of susceptible (vulnerable) prey	Population density
I	Density of infected (diseased) prey	Population density
P	Density of predator population	Population density
R	Intrinsic growth rate of susceptible prey	Time^{-1}
K	Carrying capacity of prey	Population density
γ	Fear intensity due to infected prey	(Population density)$^{-1}$
$\mathcal{U}(\gamma, I) = \frac{1}{1+\gamma I}$	Fear effect function	Dimensionless
α_1	Infection rate of prey	Time^{-1} (density)$^{-1}$
a_1	Half-saturation constant in infection function	Population density
β_1	Predator attack rate on susceptible prey	Time^{-1}
b_1	Predator attack rate on infected prey	Time^{-1}
η_1	Predator interference parameter (prey-dependent)	(Population density)$^{-1}$
μ_1	Predator interference parameter (predator-dependent)	(Population density)$^{-1}$
c	Predator conversion/assimilation efficiency	Dimensionless
D_1	Mortality rate of infected prey	Time^{-1}
D_2	Natural mortality rate of predators	Time^{-1}
ϑ	Refuge fraction available to prey	Dimensionless
$H_1E_1(S)$	Harvesting function for susceptible prey	Population density / Time
$H_2E_2(I)$	Harvesting function for infected prey	Population density / Time
H_1, H_2	Harvesting effort constants	Time^{-1}
$E_1(S), E_2(I)$	Effort response functions (increasing)	Dimensionless

tactics, has been included in predator-prey models to more accurately reflect animal behavior in the wild. Predatory animals frequently use strategies like running away or hiding from predators in the wild. These types of actions have the potential to drastically alter the dynamics of predator-prey populations. Examining the effect of fear on a prey-predator system helps researchers better understand how these behaviors affect populations of various species and how they interact. Prey populations in the biological systems mentioned above become more vulnerable as a result of the fear-inducing effects on impacted populations. The reproduction rate of susceptible prey may decline due to fear of sick prey. In this case, $S_0 \geq 0, I_0 \geq 0$, and $P_0 \geq 0$ are the criteria. The fear effect's prerequisite is

$$\mathcal{U}(\gamma, I) = \frac{1}{1+\gamma I}.$$

The amount of fear experienced by vulnerable prey due to the presence of diseased prey is described here. In this case, γ denotes the amount of dread. Considering the epidemiological interpretation of γ, the subsequent requirement is very permissible:

$$\begin{aligned} \gamma(0, I) = \mathcal{U}(\gamma, 0) &= 1, \\ \lim_{\gamma\to\infty} \mathcal{U}(\gamma, I) = \lim_{I\to\infty} \mathcal{U}(\gamma, I) &= 0, \\ \frac{\partial \mathcal{U}(\gamma, I)}{\partial \gamma} &< 0, \\ \frac{\partial \mathcal{U}(\gamma, I)}{\partial I} &< 0. \end{aligned}$$

In order to incorporate the amount of fear, we must include the term $\frac{1}{1+\gamma I}$ in model (1), where γ denotes the degree of dread. Therefore, model (1) after the fear effect is added is as follows:

$$\begin{aligned} \frac{dS}{dT} &= \frac{R\,S}{1+\gamma\,I}\left(1-\frac{S+I}{K}\right) - \frac{\alpha_1\,S\,I}{a_1+S} - \frac{\beta_1\,S\,P}{(1+\eta_1 S)\,(1+\mu_1 P)}, \\ \frac{dI}{dT} &= \frac{\alpha_1\,S\,I}{a_1+S} - D_1\,I - \frac{b_1\,I\,P}{(1+\eta_1 I)\,(1+\mu_1 P)}, \\ \frac{dP}{dT} &= -D_2\,P + \frac{c\,b_1\,I\,P}{(1+\eta_1 I)\,(1+\mu_1 P)} + \frac{c\,\beta_1\,S\,P}{(1+\eta_1 S)\,(1+\mu_1 P)}. \end{aligned} \tag{2}$$

We use the interacting species model (2) in this work with a constant prey refuge area of $0 \leq \vartheta S < S$, where ϑ is a non-negative constant. During the study, it is assumed that for a significant ecological system, $0 \leq \vartheta < 1$. Consequently, model (2) becomes eq. (3) upon the addition of the Holling type II interaction function and the constant percentage prey refuge.

$$\begin{aligned} \frac{dS}{dT} &= \frac{R\,S}{1+\gamma\,I}\left(1-\frac{S+I}{K}\right) - \frac{\beta_1\,S\,P}{(1+\eta_1 S)\,(1+\mu_1 P)} \\ &\quad - \frac{\alpha_1\,(1-\vartheta)\,S\,I}{a_1+(1-\vartheta)\,S}, \\ \frac{dI}{dT} &= \frac{\alpha_1\,(1-\vartheta)\,S\,I}{a_1+(1-\vartheta)\,S} - D_1\,I - \frac{b_1\,I\,P}{(1+\eta_1 I)\,(1+\mu_1 P)}, \\ \frac{dP}{dT} &= -D_2\,P + \frac{c\,b_1\,I\,P}{(1+\eta_1 I)\,(1+\mu_1 P)} + \frac{c\,\beta_1\,S\,P}{(1+\eta_1 S)\,(1+\mu_1 P)}. \end{aligned} \tag{3}$$

Here the conditions are $S_0 \geq 0, I_0 \geq 0$ and $P_0 \geq 0$.

In order to prevent the disease transmission/contact of illness, the number of prey is removed (harvested) by some external harvester (not by a predator). Here, we assume that the rates of removal of vulnerable prey and diseased prey are not the same. Thus, we introduce the general harvesting functions $H_1E_1(S)$ and $H_2E_2(I)$ depending upon the population density of prey individuals (vulnerable/sick prey) and satisfying the properties:

- For any $S, I > 0$, $H_1E_1(S) > 0$ and $H_2E_2(I) > 0$. In other words, if there is no infection, there is no need to harvest them, and if there is, harvesting strategies are put into place.
- The functions $H_1E_1(S)$ and $H_2E_2(I)$ are growing.

During this event, the spread of the disease is very dangerous, so they should be harvested at the same rate. Now, using this assumption of disease control, the relationship between prey harvesting and the prey and predator model is represented mathematically by a set of three coupled differential equations as follows:

$$\frac{dS}{dT} = \frac{RS}{1+\gamma I}\left(1-\frac{S+I}{K}\right) - \frac{\alpha_1(1-\vartheta)SI}{a_1+(1-\vartheta)S}$$

$$
\begin{aligned}
&- \frac{\beta_1 SP}{(1+\eta_1 S)(1+\mu_1 P)} - H_1 E_1(S),\\
\frac{dI}{dT} &= \frac{\alpha_1(1-\vartheta)SI}{a_1+(1-\vartheta)S} - D_1 I - \frac{b_1 IP}{(1+\eta_1 I)(1+\mu_1 P)}\\
&- H_2 E_2(I),\\
\frac{dP}{dT} &= \frac{cb_1 IP}{(1+\eta_1 I)(1+\mu_1 P)} + \frac{c\beta_1 SP}{(1+\eta_1 S)(1+\mu_1 P)}\\
&- D_2 P. \qquad (4)
\end{aligned}
$$

where $S_0 \geq 0, I_0 \geq 0$, and $P_0 \geq 0$ denote non-negative conditions.

2.1. Dimensionless model

In order to decrease the total number of system variables, one needs to non-dimensionalize the aforementioned model (4) by adding the dimensions $t = \lambda KT$ and $sK = S, iK = I, pK = P$. Here, λ represents a time-scaling parameter introduced during the non-dimensionalization process. The following transformations can be used to express model (4) in dimensionless form.

$$
\begin{aligned}
\frac{ds}{dt} &= \frac{r\,s}{1+\gamma\,i}(1-s-i) - \frac{\alpha(1-\vartheta)\,s\,i}{a+(1-\vartheta)\,s} - \frac{\beta\,s\,p}{(1+\eta\,s)\,(1+\mu\,p)}\\
&- h_1\,s,\\
\frac{di}{dt} &= \frac{\alpha(1-\vartheta)\,s\,i}{a+(1-\vartheta)\,s} - d\,i - \frac{b\,i\,p}{(1+\eta\,i)\,(1+\mu\,p)} - h_2\,i,\\
\frac{dp}{dt} &= -\delta\,p + \frac{c\,b\,i\,p}{(1+\eta\,i)\,(1+\mu\,p)} + \frac{c\,\beta\,s\,p}{(1+\eta\,s)\,(1+\mu\,p)}.
\end{aligned} \qquad (5)
$$

with initial conditions are $s(0) \geq 0, i(0) \geq 0, p(0) \geq 0$. Where,

$$
\begin{aligned}
r &= \frac{R}{\lambda K}, \quad \alpha = \frac{\alpha_1}{\lambda K}, \quad a = \frac{a_1}{K},\\
\beta &= \frac{\beta_1}{\lambda}, \quad \eta = \eta_1 K, \quad \mu = \mu_1 K,\\
b &= \frac{b_1}{\lambda}, \quad d = \frac{D_1}{\lambda K}, \quad \delta = \frac{D_2}{\lambda K}.
\end{aligned}
$$

3. Well posedness of the model

Theorem 1. *There exists the unique solution of model (5) if $(s(0), i(0), p(0)) > 0$ and is non-negative $\forall t \geq 0$.*

Proof. There exists a particular solution in $[0, \mathbb{I})$, where $0 < \mathbb{I} < \infty$, since the right-hand side of model (5) is continuous and locally Lipschitzian in $\mathbb{R}^3_+$.

$$
\begin{aligned}
s(t) &= s(0)\exp\left(\int_0^t \left[\frac{rs(\xi)(1-s(\xi)-i(\xi))}{1+\gamma i} - \frac{\alpha(1-\vartheta)s(\xi)i(\xi)}{a+(1-\vartheta)s(\xi)}\right.\right.\\
&\left.\left. - \frac{\beta s(\xi)p(\xi)}{(1+\eta s(\xi))(1+\mu p(\xi))} - h_1 s(\xi)\right] d\xi\right) > 0,\\
i(t) &= i(0)\exp\left(\int_0^t \left[\frac{\alpha(1-\vartheta)s(\xi)i(\xi)}{a+(1-\vartheta)s(\xi)} - \frac{bi(\xi)p(\xi)}{(1+\eta i(\xi))(1+\mu p(\xi))}\right.\right.\\
&\left.\left. - di(\xi) - h_2 i(\xi)\right] d\xi\right) > 0,\\
p(t) &= p(0)\exp\left(\int_0^t \left[\frac{cbi(\xi)p(\xi)}{(1+\eta i(\xi))(1+\mu p(\xi))} - \delta p(\xi)\right.\right.\\
&\left.\left. + \frac{c\beta s(\xi)p(\xi)}{(1+\eta s(\xi))(1+\mu p(\xi))}\right] d\xi\right) > 0,
\end{aligned}
$$

which completes the proof. □

Theorem 2. *All solutions of model (5) in $\mathbb{R}^3_+$ are uniformly bounded.*

Proof. Assume that all model parameters are nonnegative and that

$$\zeta := \min\{h_1,\ d + h_2,\ \delta\} > 0.$$

Let $(s(t), i(t), p(t))$ be any solution of model (5) with initial condition

$$s(0) = s_0 \geq 0, \qquad i(0) = i_0 \geq 0, \qquad p(0) = p_0 \geq 0,$$

and define

$$\chi(t) := s(t) + i(t) + p(t).$$

From the first equation of model (5) (dropping nonnegative loss terms and using $1 + \gamma i \geq 1$ and $1 - s - i \leq 1 - s$) we obtain the scalar inequality

$$\frac{ds}{dt} \leq rs(1-s).$$

Hence $\limsup_{t\to\infty} s(t) \leq 1$ and, in particular, $s(t)$ remains nonnegative for all $t \geq 0$. Differentiating χ along solutions of model (5) yields

$$
\begin{aligned}
\frac{d\chi}{dt} &= \frac{rs(1-s-i)}{1+\gamma i} - \frac{\alpha(1-\theta)si}{a+(1-\theta)s} - \frac{\beta sp}{(1+\eta s)(1+\mu p)} - h_1 s\\
&- \frac{bip}{(1+\eta i)(1+\mu p)} - di - h_2 i + \frac{cbip}{(1+\eta i)(1+\mu p)}\\
&+ \frac{c\beta sp}{(1+\eta s)(1+\mu p)} - \delta p.
\end{aligned}
$$

Using $0 \leq c < 1$ and collecting the predator/prey interaction terms gives the estimate

$$\frac{d\chi}{dt} \leq \frac{rs(1-s-i)}{1+\gamma i} - h_1 s - (d+h_2)i - \delta p \leq \frac{rs(1-s)}{1+\gamma i} - \zeta\,\chi(t),$$

where we used $1 + \gamma i \geq 1$ and the definition of ζ. Now for all $s \geq 0$ and $i \geq 0$ we have

$$\frac{rs(1-s)}{1+\gamma i} \leq rs(1-s) \leq \frac{r}{4},$$

since the function $s \mapsto rs(1-s)$ attains its maximum $r/4$ at $s = \frac{1}{2}$. Therefore

$$\frac{d\chi}{dt} + \zeta\,\chi \leq \frac{r}{4}.$$

Multiply by the integrating factor $e^{\zeta t}$ and integrate from 0 to t to obtain

$$\chi(t)e^{\zeta t} - \chi(0) \leq \frac{r}{4}\int_0^t e^{\zeta s}\,ds = \frac{r}{4\zeta}\left(e^{\zeta t} - 1\right).$$

Rearranging gives the explicit bound

$$\chi(t) \leq \frac{r}{4\zeta}\left(1 - e^{-\zeta t}\right) + \chi(0)e^{-\zeta t}.$$

Letting $t \to \infty$ yields the uniform bound

$$0 \leq \chi(t) \leq \frac{r}{4\zeta} \qquad \text{for all sufficiently large } t,$$

and consequently all solutions enter and remain in the compact set

$$\Omega := \left\{(s,i,p) \in \mathbb{R}^3_+ : \; s+i+p \leq \frac{r}{4\zeta} + \varepsilon\right\}$$

for any $\varepsilon > 0$. This proves that all solutions of model (5) in $\mathbb{R}^3_+$ are uniformly bounded. □

4. Stability analysis

The fixed points (s,i,p) of the model (5) may be found by solving the following equations:

$$\frac{(1-s-i)rs}{1+\gamma i} - \frac{\alpha(1-\vartheta)si}{a+(1-\vartheta)s} - \frac{\beta sp}{(1+\eta s)(1+\mu p)} - h_1 s = 0,$$
$$\frac{\alpha(1-\vartheta)si}{a+(1-\vartheta)s} - di - \frac{bip}{(1+\eta i)(1+\mu p)} - h_2 i = 0,$$
$$-\delta p + \frac{cbip}{(1+\eta i)(1+\mu p)} + \frac{c\beta sp}{(1+\eta s)(1+\mu p)} = 0.$$

We explore the possibility of biologically relevant points of equilibrium under specific parametric settings and analyze the behavior of these points in terms of stability and instability. It follows that the model (5) should possess

1. There will always be a point of trivial equilibrium. is $\mathcal{E}_0(0,0,0)$. It means the chance of species extinction cannot be denied without restriction.
2. If the development rate of the vulnerable prey exceeds the harvest rate imposed on the vulnerable prey, then there exists an equilibrium point that is free from infected prey and predator species, i.e., $\mathcal{E}_1(\frac{r-h_1}{r}, 0, 0)$, provided $r > h_1$.
3. If $(c\beta - \delta\eta(1+\mu p)) > 0$ and the imposed harvesting on susceptible prey does not exceed a particular threshold, i.e., $0 < h_1 < \left(r(1-s) - \frac{\beta}{\mu(1+\eta s)}\right)$ then there exists an infected prey free equilibrium point $\mathcal{E}_2\left(\frac{\delta(1+\mu p)}{c\beta - \delta\eta(1+\mu p)}, 0, \frac{(1+\eta s)(r(1-s)-h_1)}{\beta - \mu(1+\eta s)(r(1-s)-h_1)}\right)$ (assume $h_1 < r(1-s)$ and $s < 1$).
4. The predator-free point of equilibrium $\mathcal{E}_3 = \left(\hat{s}, \hat{i}, 0\right)$ could not be obtained explicitly due to algebraic complexity, so the number of predator-free equilibrium points depends upon the parametric values. The second component of the $\mathcal{E}_3$, i.e., $\hat{i}$, is the non-negative solution of the following equation:

$$\mathcal{Q}_1\hat{i}^2 + \mathcal{Q}_2\hat{i} + \mathcal{Q}_3 = 0,$$

where,

$$\hat{i} = \frac{-\mathcal{Q}_2 \pm \sqrt{\mathcal{Q}_2^2 - 4\mathcal{Q}_1\mathcal{Q}_3}}{2\mathcal{Q}_1},$$
$$\mathcal{Q}_1 = \gamma(1-\vartheta)^2(\alpha - d - h_2)^2,$$
$$\mathcal{Q}_2 = (1-\vartheta)(\alpha - d - h_2)[a(r + h_1\gamma)] + (1-\vartheta)(\alpha - d - h_2),$$
$$\mathcal{Q}_3 = a[ar(d+h_2) - (1-\vartheta)(r-h_1)(\alpha - d - h_2)].$$

Using the value of $\hat{i}$, the expression for the first component of $\mathcal{E}_3$ is given by $\hat{s} = \frac{a(d+h_2)}{(1-\vartheta)(\alpha-(d+h_2))}$. The number of predator-free equilibrium is governed by the $\mathcal{Q}_i (i = 1-2)$ sign.

5. The coexistence equilibrium point may be calculated by solving the predator-prey model:

$$s^* = \frac{\delta(1+\eta i^*)(1+\mu p^*) - bci^*}{bc\eta i^* + (1+\eta i^*)(c\beta - \delta\eta(1+\mu p^*))},$$
$$i^* = \frac{1}{\eta(1+\mu p^*)} \times \left[\frac{b(a+(1-\vartheta)s^*)p^*}{\alpha(1-\vartheta)s^* - (d+h_2)(a+(1-\vartheta)s^*)} - \frac{(1+\mu p^*)[\alpha(1-\vartheta)s^* - (d+h_2)(a+(1-\vartheta)s^*)]}{\alpha(1-\vartheta)s^* - (d+h_2)(a+(1-\vartheta)s^*)}\right],$$
$$p^* = \frac{(1+\eta s^*)[\frac{r(1-s^*-i^*)}{1+\gamma i^*} - \frac{\alpha(1-\vartheta)i^*}{a+(1-\vartheta)s^*} - h_1]}{\beta - \mu(1+\eta s^*)[\frac{r(1-s^*-i^*)}{1+\gamma i^*} - \frac{\alpha(1-\vartheta)i^*}{a+(1-\vartheta)s^*} - h_1]}.$$

Thus, the conditions that must exist for $\mathcal{E}^*$ are

$$\frac{\delta\eta(1+\mu p)}{c} < \beta,$$
$$d + h_2 < \frac{\alpha(1-\vartheta)s^*}{a+(1-\vartheta)s^*},$$
$$\frac{r(1-s^*-i^*)}{1+\gamma i^*} < \frac{\alpha(1-\vartheta)i^*}{a+(1-\vartheta)s^*} - h_1 + \frac{\beta}{\mu(1+\eta s^*)}.$$

At this point, we talk about the equilibrium's local stability. The following Jacobian matrix $J_{\mathcal{E}}$ is connected with the model (5). Let us assume a tiny perturbation from the equilibrium and linearize the resultant equation.

$$J(\mathcal{E}) = \begin{bmatrix} \zeta_{11} & \zeta_{12} & \zeta_{13} \\ \zeta_{21} & \zeta_{22} & \zeta_{23} \\ \zeta_{31} & \zeta_{32} & \zeta_{33} \end{bmatrix},$$

where,

$$\zeta_{11} = \frac{r(1-2s-i)}{1+\gamma i} - \frac{a\alpha(1-\vartheta)i}{(a+(1-\vartheta)s)^2} - \frac{\beta p}{(1+\eta s)^2(1+\mu p)} - h_1,$$
$$\zeta_{12} = -\frac{(\gamma(1-s)+1)rs}{(\gamma i+1)^2} - \frac{(1-\vartheta)\alpha s}{s(1-\vartheta)+a},$$
$$\zeta_{13} = -\frac{\beta s}{(1+\eta s)(1+\mu p)^2}, \quad \zeta_{21} = \frac{\alpha a(1-\vartheta)i}{(a+(1-\vartheta)s)^2},$$
$$\zeta_{23} = -\frac{bi}{(1+\mu p)^2(1+\eta i)},$$
$$\zeta_{22} = \frac{\alpha(1-\vartheta)s}{a+(1-\vartheta)s} - \frac{bp}{(1+\eta i)^2(1+\mu p)} - (d+h_2),$$
$$\zeta_{31} = \frac{\beta cp}{(1+\mu p)(1+\eta s)^2}, \quad \zeta_{32} = \frac{bcp}{(1+\mu p)(1+\eta i)^2},$$
$$\zeta_{33} = -\delta + \frac{bci}{(1+\mu p)^2(1+\eta i)} + \frac{\beta cs}{(1+\mu p)^2(1+\eta s)}.$$

- The eigenvalues of $J_{\mathcal{E}}$ at $\mathcal{E}_0(0,0,0)$ are $\lambda_1 = r - h_1$, $\lambda_2 = -(d+h_2)$, and $\lambda_3 = -\delta$.
- The eigenvalues of $J_{\mathcal{E}}$ at $\mathcal{E}_1\left(\frac{r-h_1}{r}, 0, 0\right)$ is calculated as $\lambda_1 = h_1 - r$, $\lambda_2 = \frac{\alpha(1-\vartheta)(r-h_1)}{ar+(1-\vartheta)(r-h_1)} - d - h_2$, and $\lambda_3 = -\delta + c\beta\left[\frac{r-h_1}{r+\eta(r-h_1)}\right]$.

Proposition 1. *abcdefghijklmno*

If the rate of harvesting imposed on susceptible prey is greater than their intrinsic development rate, i.e., $h_1 > r$, then the model (5) is locally stable around $\mathcal{E}_0(0,0,0)$.

(ii) If $0 < (r-h_1) < \frac{r\delta}{c\beta - \delta\eta}$ and $h_2 > d - \frac{\alpha(1-\vartheta)(r-h_1)}{ar+(1-\vartheta)(r-h_1)}$ then the model (5) is locally stable around $\mathcal{E}_1\left(\frac{r-h_1}{r}, 0, 0\right)$.

(iii) The infection-free

$$\mathcal{E}_2\left(\frac{\delta(1+\mu p)}{c\beta - \delta\eta(1+\mu p)}, 0, \frac{(1+\eta s)(r(1-s)-h_1)}{\beta - \mu(1+\eta s)(r(1-s)-h_1)}\right)$$

equilibrium point is LAS if and only if $Z_1 > 0$, $Z_3 > 0$ and $Z_1 Z_2 - Z_3 > 0$.

(iv) The predator-free $\mathcal{E}_3 = (\hat{s}, \hat{i}, 0)$ equilibrium point is LAS iff $Z_4 > 0$, $Z_6 > 0$ and $Z_4 Z_5 - Z_6 > 0$.

(v) The coexisting equilibrium $\mathcal{E}^*(s^*, i^*, p^*)$ is LAS iff $Z_7 > 0$, $Z_9 > 0$, $Z_7 Z_8 - Z_9 > 0$.

Remark 1. For details and the meaning of $Z_i (i = 1-9)$ interested readers may refer to Appendix A.1.

Theorem 3. *If $\mathcal{E}^*$ is GAS then $\mathcal{E}^*$ in $G = \{(s,i,p) : s > s^*, i > i^*$ and $p > p^*)\}$.*

Proof. For proof, refer to Appendix A.2. □

5. Bifurcation analysis

Theorem 4. *There exists a transcritical bifurcation between $\mathcal{E}_1$ and $\mathcal{E}_\infty$ if the system parameters satisfy the following criteria: $h_1 = h_1^{TC} = r$, where h_1^{TC} is the threshold value for the same.*

Proof. For proof, refer to Appendix A.3. □

Theorem 5. *We discuss the prerequisites for the coexisting equilibrium point's existence. Assume that the following requirements are satisfied by the parameters of model (5).*

1. *$J_{\mathcal{E}}|\mathcal{E}^*$ has purely imaginary eigenvalues, and $\xi_1(h_1^*)\xi_2(h_1^*) - \xi_3(h_1^*) = 0$,*
2. *$\frac{d}{dh_1}(Re(\mathcal{S}(h_1)))|_{h_1 = h_1^*} \neq 0$. Where $h_1 = h_1^*$ is the root of $\xi_1(h_1^*)\xi_2(h_1^*) - \xi_3(h_1^*) = 0$. Then, the model (5) may undergo a Hopf-bifurcation with respect to the bifurcation parameter h_1 around the equilibrium point $\mathcal{E}^*$.*

Proof. The characteristic equation corresponding to $J_{\mathcal{E}^*}$ is given as,

$$\begin{aligned}(\xi_1(h_1^*) + \xi_2(h_1^*))(\mathcal{S}(h_1^*) + \mathcal{S}^2(h_1^*))) = 0.\\ -\xi_1(h_1^*) \quad \text{and} \quad \pm i\sqrt{\xi_2(h_1^*)}.\end{aligned} \tag{6}$$

In order to obtain the Hopf-bifurcation at $h_1^* = h_1$, the following transversality criteria must be satisfied:

$$\tfrac{d}{dh_1}(Re(\mathcal{S}(h_1)))|_{h_1 = h_1^*} \neq 0.$$

For all h_1, the general roots of the above characteristic equation for model (5) are

$$\begin{aligned}\mathcal{S}_1(h_1) &= \psi_1(h_1) + i\psi_2(h_1),\\ \mathcal{S}_2(h_1) &= \psi_1(h_1) - i\psi_2(h_1),\\ \mathcal{S}_3(h_1) &= -\xi_1(h_1).\end{aligned}$$

We check the criteria

$$\tfrac{d}{dh_1}(Re(\mathcal{S}_j(h_1)))|_{h_1 = h_1^*} \neq 0, j = 1, 2.$$

Let, $\mathcal{S}_1(h_1) = \psi_1(h_1) + i\psi_2(h_1)$ in eq. (6), we get $\sigma_1(h_1) + i\sigma_2(h_1) = 0$, where

$$\begin{aligned}\sigma_1(h_1) &= \xi_2(h_1)\xi_1(h_1) + \xi_2(h_1)\psi_1(h_1) - \xi_1(h_1)\psi_2^2(h_1)\\ &\quad - 3\psi_1(h_1)\psi_2^2(h_1) + \xi_1(h_1)\psi_1^2(h_1) + \psi_1^3(h_1),\\ \sigma_2(h_1) &= \xi_2(h_1)\psi_2(h_1) - \psi_2^3(h_1) + 2\psi_2(h_1)\psi_1(h_1)\xi_1(h_1)\\ &\quad + 3\psi_2^2(h_1)\psi_2(h_1),\end{aligned}$$

$$\frac{d\sigma_1}{dh_1} = \psi_1^{'}(h_1)\varrho_1(h_1) - \psi_2^{'}(h_1)\varrho_2(h_1) + \varrho_3(h_1) = 0, \tag{7}$$

$$\frac{d\sigma_2}{dh_1} = \psi_1^{'}(h_1)\varrho_2(h_1) + \psi_2^{'}(h_1)\varrho_1(h_1) + \varrho_4(h_1) = 0, \tag{8}$$

$$\begin{aligned}\varrho_4(h_1) &= \psi_2(h_1)\xi_2^{'}(h_1) + 2\psi_1(h_1)\psi_2(h_1)\xi_1^{'}(h_1),\\ \varrho_3(h_1) &= \xi_2^{'}(h_1)\psi_1(h_1) + \xi_3^{'}(h_1) - \psi_2^2(h_1)\xi_1^{'}(h_1)\\ &\quad + \psi_1^2(h_1)\xi_1^{'}(h_1),\\ \varrho_2(h_1) &= 2\psi_2(h_1)\xi_1(h_1) + 6\psi_1(h_1)\psi_2(h_1),\\ \varrho_1(h_1) &= \xi_2(h_1) - 3\psi_2^2(h_1) + 2\psi_1(h_1)\xi_1(h_1) + 3\psi_1^2(h_1).\end{aligned}$$

By multiplying eqs. (7) and (8) in $\varrho_1(h_1)$ and $\varrho_2(h_1)$, respectively,

$$-\frac{\varrho_1(h_1)\varrho_3(h_1) + \varrho_2(h_1)\varrho_4(h_1)}{\varrho_1^2(h_1) + \varrho_2^2(h_1)} = \psi_1^{'}(h_1). \tag{9}$$

Substituting $\psi_1(h_1) = 0$ and $\psi_2(h_1) = \sqrt{\xi_2(h_1)}$ at $h_1 = h_1^*$ on $\varrho_4(h_1)$, $\varrho_3(h_1)$, $\varrho_2(h_1)$ and $\varrho_1(h_1)$ we obtain

$$\begin{aligned}-2\xi_2(h_1^*) &= \varrho_1(h_1^*),\\ 2\sqrt{\xi_2(h_1^*)}\xi_1(h_1^*) &= \varrho_2(h_1^*),\\ -\xi_2(h_1^*)\xi_1^{'}(h_1^*) + \xi_3^{'}(h_1^*) &= \varrho_3(h_1^*),\\ \sqrt{\xi_2(h_1^*)}\xi_2^{'}(h_1^*) &= \varrho_4(h_1^*).\end{aligned}$$

The eq. (9), implies

$$\psi^{'}(h_1^*) = \tfrac{\xi_3^{'}(h_1^*) - (\xi_1(h_1^*)\xi_2^{'}(h_1^*) + \xi_1^{'}(h_1^*)\xi_2(h_1^*))}{2(\xi_2^2(h_1^*) + \xi_1^2(h_1^*))}, \tag{10}$$

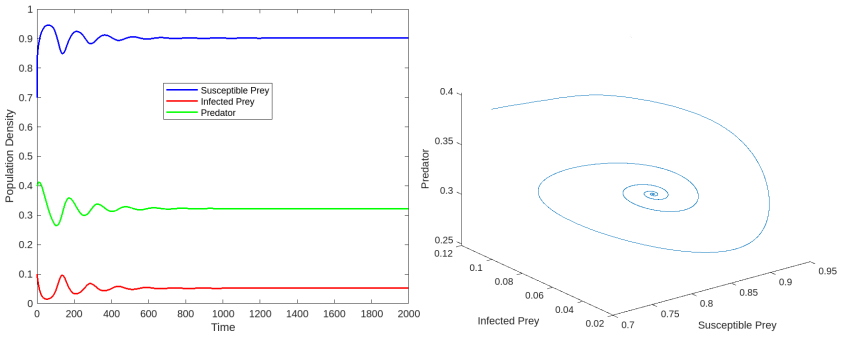

(a) (b)

Figure 1. The solution of model (5). The subfigure (a) shows the time evolution of the population densities. (b) shows the phase portrait around E^*.

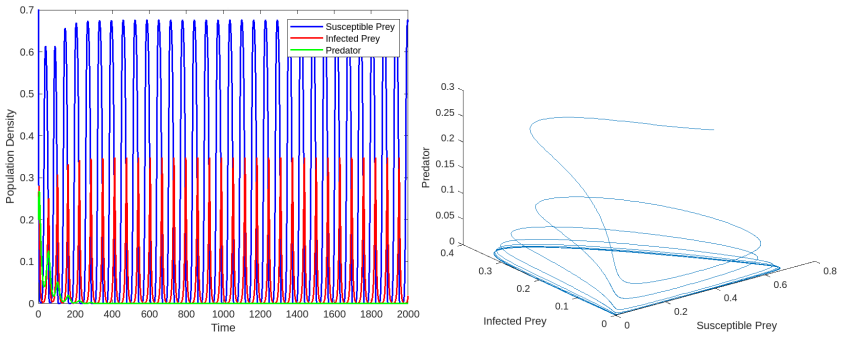

(a) (b)

Figure 2. The solution of the model (5) shows the time evolution of the population densities, and the phase portrait diagram is unstable.

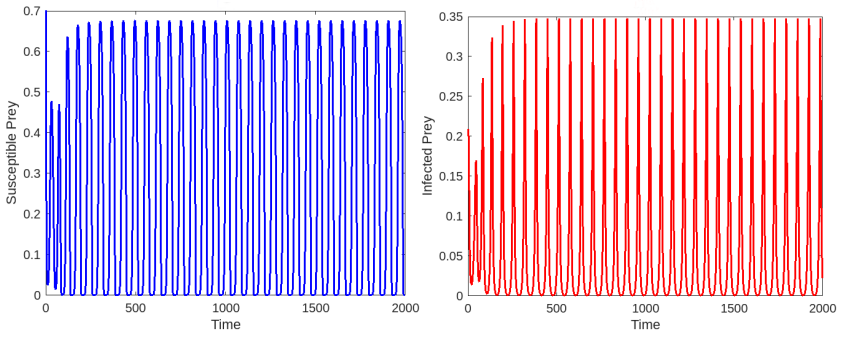

(a) (b)

Figure 3. The time evolution for model (5) is non-stationary.

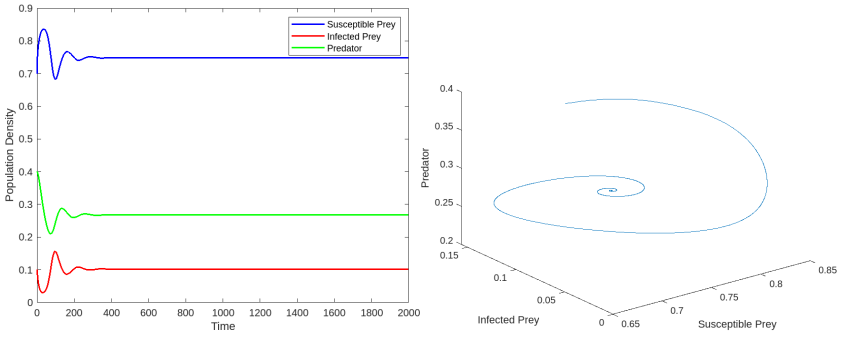

(a) (b)

Figure 4. The solution of model (5). The subfigure (a) shows the time evolution of the population densities. (b) shows the phase portrait around E^*. When ($\vartheta = 0.2$, and $h_1 = 0.2$.)

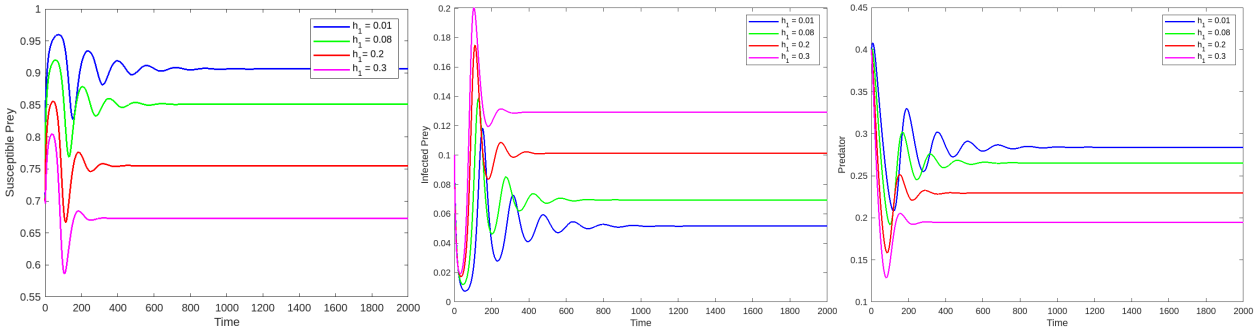

(a) (b) (c)

Figure 5. Effects of hunting cooperation with different values for $h_1 = 0.01, 0.08, 0.2, 0.3$ and $\vartheta = 0.2$.

Table 2. Parameters used in the model and their sources

Parameter	Description	Values	Source / Reference
r	Prey intrinsic growth rate	2	Assumed
α	Infection transmission rate	0.7	[17]
a	Saturation constant for infection	0.6	[33]
β	Predation rate (susceptible prey)	0.2	[33]
γ	Fear parameter (or effect of infected)	0.2	[33]
ϑ	Refuge coefficient	0.3	[33]
η, μ	Saturation constants in predation	0.1 (each)	[32]
h_1, h_2	Harvesting rates for S and I	0.2, 0.1	[32]
d	Death / recovery rate of infected	0.1	[32]
b	Predation rate (infected prey)	0.55	Assumed
δ	Predator death rate	0.1	[32]
c	Conversion efficiency (prey predator)	0.5	[47]

If $-(\xi_2^{'}(h_1^*)\xi_1(h_1^*) + \xi_1^{'}(h_1^*)\xi_2(h_1^*)) + \xi_3^{'}(h_1^*) \neq 0$, which implies that

$$\frac{d}{dh_1}(Re(\mathcal{S}_j(h_1)))|_{h_1=h_1^*} = \xi^{'}(h_1^*) \neq 0.j = 1, 2,$$
$$\mathcal{S}_3(h_1^*) = -\xi_1(h_1^*) \neq 0$$

If $-(\xi_2^{'}(h_1^*)\xi_1(h_1^*) + \xi_1^{'}(h_1^*)\xi_2(h_1^*)) + \xi_3^{'}(h_1^*) \neq 0$, it is guaranteed that the transversality criterion is satisfied, so the Hopf-bifurcation at $h_1 = h_1^*$ is reached in model (5). Our analysis shows that the system undergoes a supercritical Hopf bifurcation. Specifically, the bifurcating periodic solutions emerging at the critical parameter value are stable, confirming that the Hopf bifurcation is supercritical. □

6. Numerical Analysis

Using the quantitative findings discussed in this part, we show our numerical results for a model (5) that includes harvest, refuge, and fear effects. However, since our model is an integer-order ODE system, all simulations in this study were carried out exclusively with the standard RK4 scheme. Table 2 shows the parametric values of the model. The numerical simulations were performed using a fixed time step of 0.01, initial conditions used were (S, I, P) = (50,5,10) and oscillatory mode up to 800-time units.

Figure 1 describes the changing behavior of the solution state with respect to time at E^* of the model (5). To ensure biological relevance, all numerical simulations were carried out using parameter values obtained from previously published eco-epidemiological studies. Specifically, the values of r, α, β, b, c, d, δ, γ, h_1, h_2 and the saturation constants were selected based on empirical or widely used modeling ranges reported [17, 32, 33, 47]. These studies provide parameter estimates for predator–prey interactions, disease transmission within prey populations, and predator functional responses that are consistent with the structure of our model. The chosen values, therefore, reflect biologically plausible ranges and ensure that the numerical results are grounded in established literature. In Figure 1a, all three populations survive in oscillatory mode up to 800-time units, and the later system approaches a stable coexisting point of equilibrium $(E^*(0.727601, 0.121224, 0.228488)$. Figure 1b depicts the phase graph that goes with Figure 1a.

When the development rate of vulnerable prey declines, i.e., $r = 1$, the model (5) oscillates at E^*, as illustrated in Figure 2a. Figure 2b represents the corresponding phase diagrams of Figure 2a. For the model (5), the corresponding time-analysis of vulnerable prey and diseased prey are shown in Figures 3a and 3b. Figure 4, we investigate the harvesting parameters individually. If $h_1 = 0.2$ and $h_2 = 0.1$, then the model (5) is LAS about $E^*(0.727601, 0.121224, 0.228488)$, which is shown in Figure 4. Figures 5a to 5c show that as the rate of harvesting vulnerable prey is raised, the number of diseased prey increases and the population of vulnerable prey and predators falls.

The hues blue, red, and green in Figure 6 stand for vulnerable prey, diseased prey, and predator populations, respectively. Here, Figure 6a depicts the oscillatory dynamics tending to a sustainable steady state as the harvesting rate h_1 increases. Further, as we change the value of $h_1 = 0.5$, the oscillatory behavior (Figures 6a to 6c) are the bifurcation diagrams with respect to harvesting parameter h_1. Next, we investigate the effect of varying the refuge rate ϑ. It is LAS, as shown in Figure 7. For

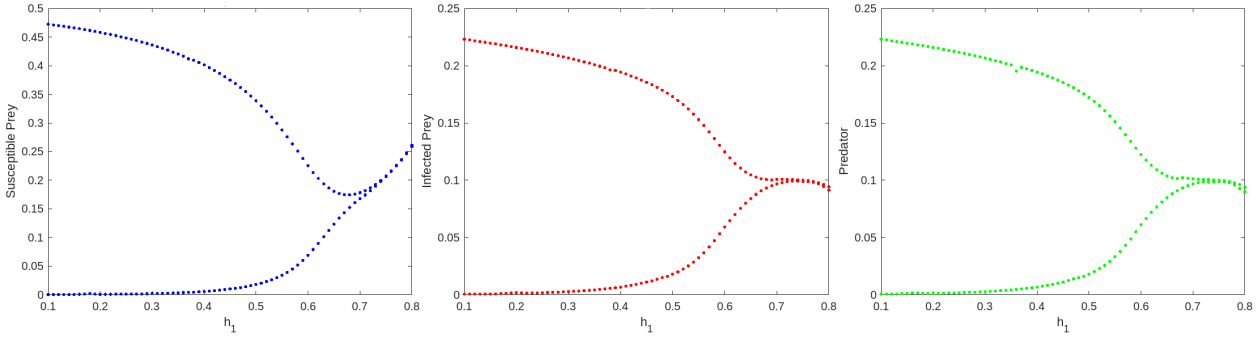

Figure 6. Bifurcation diagrams of model (5) with respect to the system parameter h_1.

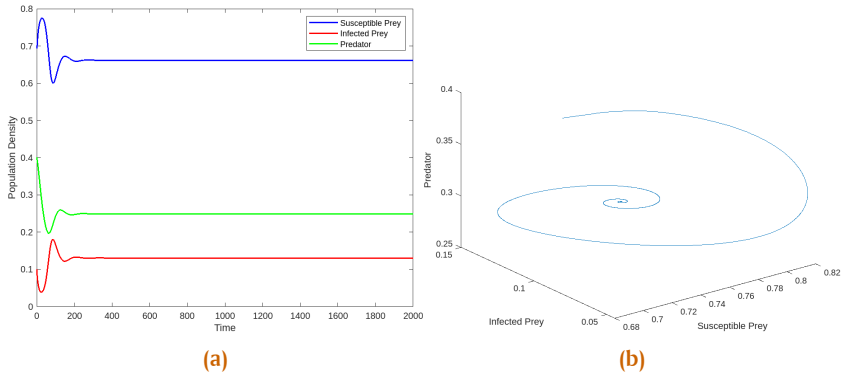

Figure 7. The solution of model (5). The subfigure (a) shows the time evolution of the population densities. (b) shows the phase portrait around E^*. When $h_1 = 0.2$, and $\vartheta = 0.1$.

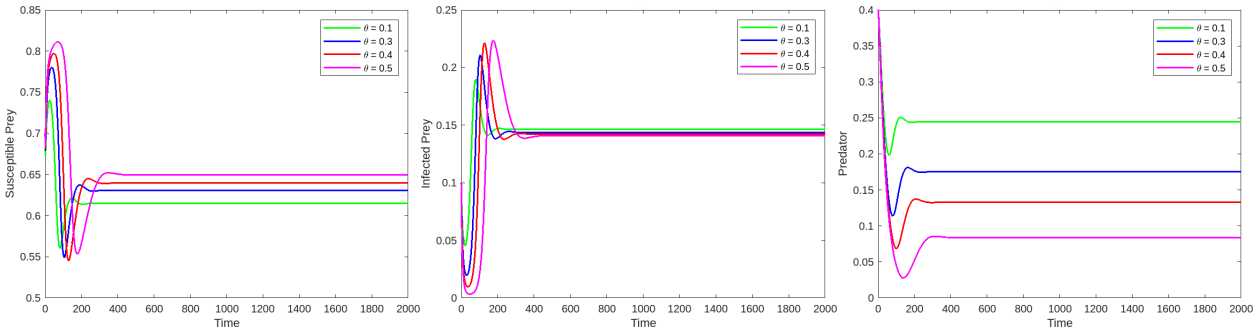

Figure 8. Effects of refuge with different values for $\vartheta = 0.1, 0.3, 0.4, 0.5$. and $h_1 = 0.2$

$0.1 < \vartheta < 0.5$, respectively, the coexisting point of equilibrium $E^*(0.727601, 0.121224, 0.228488)$ exists. According to Figure 8, when the refuge rate of susceptible prey is raised, the proportion of susceptible prey increases and the proportion of sick prey decreases.

6.1. *Optimal harvesting strategy*

The model contains two harvesting parameters, h_1 (harvesting of susceptible prey) and h_2 (harvesting of infected prey). Numerical simulations reveal a consistent pattern regarding their ecological roles. First, increasing the infected-prey harvesting rate h_2 substantially reduces the size of the infected class $i(t)$, lowers the effective transmission potential, and enlarges the parameter region in which the disease-free equilibrium becomes stable. Thus, harvesting infected individuals acts as an effective disease-control mechanism. Second, excessive harvesting of susceptible prey (h_1 large) destabilizes the system by driving the susceptible population below the level required to suppress transmission, thereby facilitating disease persistence and weakening predator–prey coexistence. Finally, a balanced regime moderate h_1 together with sufficiently large h_2 produces the most desirable outcome: a healthy susceptible population, suppressed infection, and stable predator persistence. Therefore, the model indicates that the *optimal harvesting strategy* is to apply intensive harvesting to infected prey (large h_2) while applying only light or moderate harvesting to susceptible prey (small to moderate

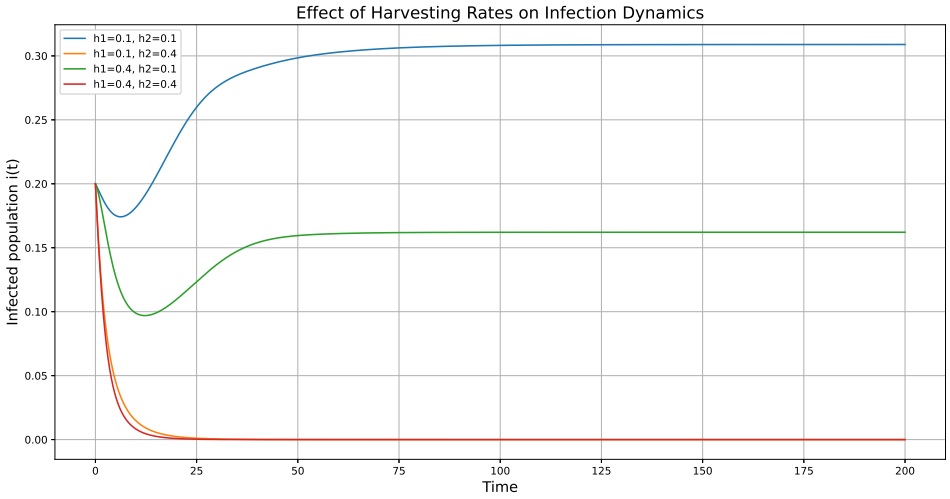

Figure 9. Effects of Harvesting on infection dynamics

h_1), ensuring both disease control and ecological stability. The effects of optimal harvesting on susceptible and infected populations, as well as the bifurcation behavior due to harvesting, are shown in Figures 5, 6 and 9.

6.2. Biological observations of Fear, Refuge, Disease Transmission, and Harvesting

The numerical simulations reveal several important biological insights arising from the combined influences of fear, refuge, disease transmission, and harvesting. The fear parameter reduces the effective contact rate between susceptible and infected prey, thereby lowering infection pressure. When fear exceeds a critical threshold, the infected population declines to zero, enlarging the domain of disease-free stability. Similarly, the refuge parameter protects a portion of susceptible prey from both predation and infection. Increasing refuge decreases predation pressure and disease transmission, ultimately preventing the persistence of infection. The combined effects of fear, refuge, and appropriate predator harvesting guide the system toward a healthy, disease-free state. These numerical observations support and complement the theoretical results established in the preceding theorems.

7. Discussions and Conclusion

An eco-epidemic model deals with the interdependent environments of populations that transmit disease. Different control measures and techniques are used to control the disease; harvesting is one of them.It is observed that harvesting plays a very crucial role in preventing the transmission of infectious illnesses. Therefore, it becomes more significant to analyze the impact of harvesting on a system when the disease is prevalent. An eco-epidemic model incorporating prey harvesting has been presented in the current investigation. We have discussed the impact of the rate of harvesting by considering linear harvesting functions. A thorough investigation of the model reveals a wide range of complex behaviors. We started out by talking about the positivity and boundedness of the suggested model system's solutions. There are five different sorts of equilibria states that can arise for model (5) under different harvesting schemes: trivial, disease and predator-free, without infection, predator-free, and coexistence of species. The stability conditions of different existing states majorly depend on disease control parameters h_1 and h_2. It could be observed in Proposition 3 for linear harvesting. To determine whether a disease has the potential to propagate and continue spreading or if it will eventually fade out and cease to exist, the reproduction number is calculated. The various bifurcations occur for model (5) under harvesting schemes. During harvesting, the transcritical bifurcation (Theorem 4) and Hopf bifurcation (Theorem 5) are experienced by the model (5) when the harvesting parameter h_1 is varied. Furthermore, the quantitative results pertaining to the harvesting operations are carried out. The positivity ensures that the population cannot be negative, while the limitation of the solution can be understood as a natural limit to growth due to limited resources. Furthermore, we observe that, in the long run, the predator population will die out of the system if the overall growth of the predator does not exceed its natural mortality rate. The trivial point of equilibrium depicts that there is no predator when there is no prey (susceptibility and infection). The infection-free equilibrium point implies that vulnerable prey and predators survive when illness is not present. The equilibrium point without a predator shows that there are susceptible and infected prey when there is no predator. The coexisting states depict that in the presence of disease, the survival of species is possible. Further, the local stability of various states could be managed by varying the imposed control parameters. A transcritical bifurcation in a system states that stability could be exchanged between two existing states by governing the bifurcation parameter (refer to Theorem 4). In the context of our study, a transcritical bifurcation underscores the capacity for sudden alterations in ecological patterns. Based on the above description, we can infer that an appropriate harvesting technique is helpful in controlling the infection. By varying the rate of harvesting, one could eradicate the disease. In summary, this study offers several threshold values for which the system can support a higher number of susceptible prey in the presence of harvesting. However, the future direction of research looks very attractive.

In the future, we would like to perform a detailed analysis of the model and investigate the impact of delay on the model dynamics. These future studies will yield exciting results related to the effect of delay.

Author Contributions. **Divya, A.**: Investigation, Writing- Original draft preparation, Methodology, Validation. **Sivabalan, M.**: Supervision, Writing - Review & Editing. **Yavuz, M.**: Supervision, Writing - Review & Editing. **Ashwin, A.**: Formal analysis, Data collection. **Pradeep, M. S.**: Conceptualization, Writing - Review & Editing.

Acknowledgement. I wish to extend my special thanks to Sri Ramakrishna Mission Vidyalaya College of Arts and Science for providing all the support and research facilities. The authors also express gratitude to the editors and reviewers who have contributed to improving the quality of this manuscript.

Funding. This research was no external funding.

Conflict of interest. The authors declare that there are no conflicts of interest in this paper.

Data availability. No data associated with the manuscript.

References

[1] S. Allesina and S. Tang, "Stability Criteria for Complex Ecosystems," *Nature*, vol. 483, no. 7388, pp. 205–208, 2012. DOI:10.1038/nature10832

[2] M. T. Alves and F. M. Hilker, "Hunting cooperation and Allee effects in predators," *Journal of Theoretical Biology*, vol. 419, pp. 13–22, 2017. DOI:10.1016/j.jtbi.2017.02.002

[3] R. M. Anderson and R. M. May, "The invasion, persistence and spread of infectious diseases within animal and plant communities," *Philosophical Transactions of the Royal Society of London. Series B, Biological Sciences*, vol. 314, no. 1167, pp. 533–570, 1986. DOI:10.1098/rstb.1986.0072

[4] N. Bairagi, S. Chaudhuri, and J. Chattopadhyay, "Harvesting as a disease control measure in an eco-epidemiological system – a theoretical study," *Mathematical Biosciences*, vol. 217, no. 2, pp. 134–144, 2009. DOI:10.1016/j.mbs.2008.11.002

[5] A. A. Berryman, "The origins and evolution of predator–prey theory," *Ecology*, vol. 73, no. 5, pp. 1530–1535, 1992. DOI:10.2307/1940005

[6] S. Biswas, "Mathematical modeling of visceral leishmaniasis and control strategies," *Chaos, Solitons & Fractals*, vol. 104, pp. 546–556, 2017. DOI:10.1016/j.chaos.2017.09.005

[7] L. Boulaasair, M. Yavuz, and H. Bouzahir, "Asymptotic Analysis of Poverty Dynamics via Feller Semigroups," *Mathematics*, vol. 13, no. 13, p. 2120, 2025. DOI:10.3390/math13132120

[8] H. S. Panigoro *et al.*, "Bifurcations on a discrete-time SIS epidemic model with saturated infection rate," *Bulletin of Biomathematics*, vol. 2, no. 2, pp. 182–197, 2025. DOI:10.59292/bulletinbiomath.2024008

[9] F. Brauer and A. C. Soudack, "Coexistence properties of some predator–prey systems under constant rate harvesting and stocking," *Journal of Mathematical Biology*, vol. 12, pp. 101–114, 1982. DOI:10.1007/BF00275206

[10] C.-W. Chang *et al.*, "A modified two-step optimal iterative method for solving nonlinear models in one and higher dimensions," *Mathematics and Computers in Simulation*, vol. 229, pp. 448–467, 2025. DOI:10.1016/j.matcom.2024.09.021

[11] K. S. Chaudhuri, "A bioeconomic model of harvesting a multispecies fishery," *Ecological Modelling*, vol. 32, no. 4, pp. 267–279, 1986. DOI:10.1016/0304-3800(86)90091-8

[12] F. Courchamp, L. Berec, and J. Gascoigne, "*Allee Effects in Ecology and Conservation*." Oxford: Oxford University Press, 2008. DOI:10.1093/acprof:oso/9780198570301.001.0001

[13] P. H. Crowley and E. K. Martin, "Functional responses and interference within and between year classes of a dragonfly population," *Journal of the North American Benthological Society*, vol. 8, no. 3, pp. 211–221, 1989. DOI:10.2307/1467324

[14] M. I. S. da Silveira Costa, "Harvesting induced fluctuations: insights from a threshold management policy," *Mathematical Biosciences*, vol. 205, no. 1, pp. 77–82, 2007. DOI:10.1016/j.mbs.2006.03.023

[15] A. P. Dobson and R. M. May, "The effects of parasites on fish populations—theoretical aspects," *International Journal for Parasitology*, vol. 17, no. 2, pp. 363–370, 1987. DOI: 10.1016/0020-7519(87)90111-1

[16] Q. Dong, W. Ma, and M. Sun, "The asymptotic behavior of a chemostat model with Crowley–Martin type functional response and time delays," *Journal of Mathematical Chemistry*, vol. 51, no. 5, pp. 1231–1248, 2013. DOI: 10.1007/s10910-012-0138-z

[17] R. Geetha *et al.*, "Biodiversity and ecosystem stability in a four-species prey–predator food chain with meta-communities," *AIMS Bioengineering*, vol. 12, no. 4, pp. 530–555, 2025. DOI:10.3934/bioeng.2025025

[18] L. N. Guin *et al.*, "Pattern dynamics of a reaction–diffusion predator–prey system with both refuge and harvesting," *International Journal of Biomathematics*, vol. 14, no. 1, p. 2050084, 2021. DOI:10.1142/S1793524520500849

[19] R. Han *et al.*, "Dynamical response of a reaction–diffusion predator–prey system with cooperative hunting and prey refuge," *Journal of Statistical Mechanics: Theory and Experiment*, vol. 2022, no. 10, p. 103502, 2022. DOI:10.1088/1742-5468/ac946d

[20] C. S. Holling, "The functional response of predators to prey density and its role in mimicry and population regulation," *The Memoirs of the Entomological Society of Canada*, vol. 97, no. S45, pp. 5–60, 1965. DOI:10.4039/entm9745fv

[21] Y. Huang, F. Chen, and L. Zhong, "Stability analysis of a prey–predator model with Holling type III response function incorporating a prey refuge," *Applied Mathematics and Computation*, vol. 182, no. 1, pp. 672–683, 2006. DOI:10.1016/j.amc.2006.04.030

[22] H. Joshi and M. Yavuz, "A novel fractional-order model and analysis of cancer-immune system interaction in an avascular environment with an efficient control mechanism," *Journal of Computational and Applied Mathematics*, vol. 473, p. 116888, 2025. DOI:10.1016/j.cam.2025.116888

[23] W. O. Kermack and A. G. McKendrick, "A contribution to the mathematical theory of epidemics," *Proceedings of the Royal Society of London. Series A*, vol. 115, no. 772, pp. 700–721, 1927. DOI:10.1098/rspa.1927.0118

[24] A. J. Lotka, "*Elements of Mathematical Biology*." New York: Dover Publications, 1956.

[25] A. J. Lotka, "*Elements of Physical Biology*." Baltimore: Williams & Wilkins, 1925.

[26] P. Luis *et al.*, "Implementation of non-standard finite difference on a predator–prey model considering cannibalism on predator and harvesting on prey," *Jambura Journal of Biomathematics (JJBM)*, vol. 6, no. 1, pp. 35–43, 2025. DOI:10.37905/jjbm.v6i1.30550

[27] Z. Ma *et al.*, "The effect of prey refuge in a patchy predator–prey system," *Mathematical Biosciences*, vol. 243, no. 1, pp. 126–130, 2013. DOI:10.1016/j.mbs.2013.02.011

[28] K. Makwana, R. Babu A., and B. P. S. Jadon, "Effect of toxicant on one prey and two competing predators with Beddington–DeAngelis functional response," *Jambura Journal of Biomathematics (JJBM)*, vol. 6, no. 1, pp. 44–59, 2025. DOI:10.37905/jjbm.v6i1.30686

[29] G. Mandal *et al.*, "Impact of fear on a tri-trophic food chain model with supplementary food source," *International Journal of Dynamics and Control*, vol. 11, no. 5, pp. 2127–2160, 2023. DOI:10.1007/s40435-022-01104-2

[30] A. Martin and S. Ruan, "Predator–prey models with delay and prey harvesting," *Journal of Mathematical Biology*, vol. 43, pp. 247–267, 2001. DOI:10.1007/s002850100095

[31] T. Megala *et al.*, "Dynamics of re-infection in a hepatitis B virus epidemic model with constant vaccination and preventive measures," *Journal of Applied Mathematics and Computing*, vol. 71, pp. 5669–5695, 2025. DOI:10.1007/s12190-025-02431-1

[32] T. Megala *et al.*, "A diseased three-species harvesting food web model with various response functions," *Biology and Life Sciences Forum*, vol. 30, no. 1, p. 17, 2024. DOI:10.3390/IOCAG2023-16876

[33] T. Megala *et al.*, "A role of fear on diseased food web model with multiple functional response," *Physical Biology*, vol. 22, no. 1, p. 016004, 2024. DOI:10.1088/1478-3975/ad9261

[34] D. Mukherjee, "The effect of prey refuges on a three species food chain model," *Differential Equations and Dynamical Systems*, vol. 22, no. 4, pp. 413–426, 2014. DOI:10.1007/s12591-013-0196-0

[35] P. A. Naik *et al.*, "Advancing Lotka–Volterra system simulation with variable fractional order Caputo derivative for enhanced dynamic analysis," *J. Appl. Anal. Comput.*, vol. 15, no. 2, pp. 1002–1019, 2025. DOI:10.11948/20240243

[36] S. Ahmad *et al.*, "On the analysis of a fractional tuberculosis model with

the effect of an imperfect vaccine and exogenous factors under the Mittag–Leffler kernel," *Fractal and Fractional*, vol. 7, no. 7, article 526, 2023. DOI:10.3390/fractalfract7070526
[37] P. A. Naik *et al.*, "Fractional insights in tumor modeling: an interactive study between tumor carcinogenesis and macrophage activation," *Advanced Theory and Simulations*, vol. 8, no. 7, p. 2401477, 2025. DOI:10.1002/adts.202401477
[38] H. Nasir and A. A. M. Daud, "Global dynamics and sensitivity analysis of a diabetic population model with two-time delays," *Mathematical Modelling and Numerical Simulation with Applications*, vol. 5, no. 1, pp. 198–233, 2025. DOI:10.53391/mmnsa.1545744
[39] C. Nkeki and I. Mbarie, "On a mathematical model and the efficacy of control measures on the transmission dynamics of chickenpox," *Bulletin of Biomathematics*, vol. 3, no. 1, pp. 37–61, 2025. DOI:10.59292/bulletinbiomath.1707079
[40] A. Padder *et al.*, "Dynamical analysis of a vector-borne disease model with control function strategies," *Discover Applied Sciences*, vol. 7, no. 9, p. 1031, 2025. DOI:10.1007/s42452-025-07644-4
[41] S. Qureshi *et al.*, "Use of fractional calculus to avoid divergence in Newton-like solver for solving one-dimensional nonlinear polynomial-based models," *Communications in Nonlinear Science and Numerical Simulation*, vol. 143, p. 108631, 2025. DOI:10.1016/j.cnsns.2025.108631
[42] S. Samaddar, M. Dhar, and P. Bhattacharya, "Effect of fear on prey–predator dynamics: Exploring the role of prey refuge and additional food," *Chaos: An Interdisciplinary Journal of Nonlinear Science*, vol. 30, no. 6, p. 063129, 2020. DOI:10.1063/5.0006968
[43] S. Sarwardi, P. K. Mandal, and S. Ray, "Analysis of a competitive prey–predator system with a prey refuge," *Biosystems*, vol. 110, no. 3, pp. 133–148, 2012. DOI:10.1016/j.biosystems.2012.08.002
[44] T. A. Shamaki, "An optimal control strategy for cerebrospinal meningitis in Yobe State, Nigeria: a mathematical modeling approach," *Bulletin of Biomathematics*, vol. 3, no. 2, pp. 192–211, 2025. DOI:10.59292/bulletinbiomath.1724391
[45] A. Sih, "Prey refuges and predator–prey stability," *Theoretical Population Biology*, vol. 31, no. 1, pp. 1–12, 1987. DOI:10.1016/0040-5809(87)90019-0
[46] M. K. Singh and P. Poonam, "Bifurcation analysis of an additional food-provided predator–prey system with anti-predator behavior," *Mathematical Modelling and Numerical Simulation with Applications*, vol. 5, no. 1, pp. 38–64, 2025. DOI:10.53391/mmnsa.1496827
[47] M. S. Pradeep, T. N. Gopal, and A. Yasotha, "Dynamics and bifurcation analysis of an eco-epidemiological model in a Crowley–Martin functional response with the impact of fear," *Engineering Proceedings*, vol. 56, no. 1, p. 329, 2023. DOI:10.3390/ASEC2023-16250
[48] G. T. Skalski and J. F. Gilliam, "Functional responses with predator interference: viable alternatives to the Holling type II model," *Ecology*, vol. 82, no. 11, pp. 3083–3092, 2001. DOI:10.1890/0012-9658(2001)082[3083:FRWPIV]2.0.CO;2
[49] J. P. Tripathi, D. Tripathi, S. Mandal, and M. D. Shrimali, "Cannibalistic enemy–pest model: effect of additional food and harvesting," *Journal of Mathematical Biology*, vol. 87, no. 4, p. 58, 2023. DOI:10.1007/s00285-023-01991-9
[50] R. K. Upadhyay and R. K. Naji, "Dynamics of a three species food chain model with Crowley–Martin type functional response," *Chaos, Solitons & Fractals*, vol. 42, no. 3, pp. 1337–1346, 2009. DOI:10.1016/j.chaos.2009.03.020
[51] R. K. K. Upadhyay, S. N. N. Raw, and V. Rai, "Dynamical complexities in a tritrophic hybrid food chain model with Holling type II and Crowley–Martin functional responses," *Nonlinear Analysis: Modelling and Control*, vol. 15, no. 3, pp. 361–375, 2010. DOI:10.15388/NA.15.3.14331
[52] V. Volterra, "Variations and fluctuations of the number of individuals in animal species living together," *Animal Ecology*, vol. 3, no. 1, pp. 3–51, 1928. DOI:10.1093/icesjms/3.1.3
[53] J. Wang, Y. Cai, S. Fu, and W. Wang, "The effect of the fear factor on the dynamics of a predator–prey model incorporating the prey refuge," *Chaos: An Interdisciplinary Journal of Nonlinear Science*, vol. 29, no. 8, p. 083109, 2019. DOI:10.1063/1.5111121

Appendix

A.1

The Jacobian matrix $J_{\mathcal{E}}$ at

$$\mathcal{E}_2\left(\frac{\delta(1+\mu p)}{c\beta-\delta\eta(1+\mu p)},0,\frac{(1+\eta s)(r(1-s)-h_1)}{\beta-\mu(1+\eta s)(r(1-s)-h_1)}\right)$$

is given byh

$$J(\mathcal{E}_2)=\begin{bmatrix}a_{11}&a_{12}&a_{13}\\a_{21}&a_{22}&a_{23}\\a_{31}&a_{32}&a_{33}\end{bmatrix},$$

$$\begin{aligned}
a_{11}&=r(1-2\bar{s})-\frac{\beta\bar{p}}{(1+\eta\bar{s})^2(1+\mu\bar{p})}-h_1,\\
a_{12}&=-\bar{s}r(2-\bar{s})+\frac{\alpha\bar{s}(1-\vartheta)}{a+(1-\vartheta)\bar{s}},\\
a_{13}&=-\frac{\beta\bar{s}}{(1+\eta\bar{s})(1+\mu\bar{p})^2},\quad a_{21}=0,\\
a_{22}&=\frac{\alpha(1-\vartheta)\bar{s}}{a+(1-\vartheta)\bar{s}}-\frac{b\bar{p}}{1+\mu\bar{p}}-(d+h_2),\quad a_{23}=0,\\
a_{31}&=\frac{\beta c\bar{p}}{(1+\eta\bar{s})^2(1+\mu\bar{p})},\quad a_{32}=-\frac{bc\bar{p}}{1+\mu\bar{p}},\\
a_{33}&=-\delta+\frac{\beta c\bar{s}}{(1+\eta\bar{s})(1+\mu\bar{p})^2}.
\end{aligned}$$

The characteristic equation associated with the above matrix is

$$\lambda^3+Z_1\lambda^2+Z_2\lambda+Z_3=0,$$

where,

$$\begin{aligned}
Z_1&=-(a_{11}+a_{22}+a_{33}),\ Z_2=a_{22}a_{33}+a_{11}a_{33}-a_{13}a_{31}+a_{11}a_{22},\\
Z_3&=-\det(J_{\mathcal{E}}|\mathcal{E}_2)=-[a_{11}a_{22}a_{33}-a_{13}a_{22}a_{31}].
\end{aligned}$$

Now, using Routh-Hurwitz criterion, $\mathcal{E}_2$ is locally asymptotically stable iff $Z_1>0$, $Z_3>0$, and $Z_1Z_2-Z_3>0$.
The Jacobian matrix $J_{\mathcal{E}}$ at $\mathcal{E}_3=(\hat{s},\hat{i},0)$ associated with the model (5) is given as:

$$J(\mathcal{E}_3)=\begin{bmatrix}b_{11}&b_{12}&b_{13}\\b_{21}&b_{22}&b_{23}\\b_{31}&b_{32}&b_{33}\end{bmatrix}$$

$$\begin{aligned}
b_{11}&=\frac{r(1-2\hat{s}-\hat{i})}{1+\gamma\hat{i}}-\frac{a\alpha(1-\vartheta)\hat{i}}{(a+(1-\vartheta)\hat{s})^2}-h_1,\\
b_{12}&=-\hat{s}\left[\frac{r(2-\hat{s})}{(1+\gamma\hat{i})^2}+\frac{\alpha(1-\vartheta)}{a+(1-\vartheta)\hat{s}}\right],\\
b_{13}&=-\frac{\beta\hat{s}}{1+\eta\hat{s}},\quad b_{21}=\frac{\alpha a(1-\vartheta)\hat{i}}{(a+(1-\vartheta)\hat{s})^2},\\
b_{22}&=\frac{\alpha(1-\vartheta)\hat{s}}{a+(1-\vartheta)\hat{s}}-(d+h_2),\quad b_{23}=-\frac{b\hat{i}}{1+\eta\hat{i}},\\
b_{31}&=0,\quad b_{32}=0,\quad b_{33}=-\delta+\frac{bc\hat{i}}{1+\eta\hat{i}}+\frac{\beta c\hat{s}}{1+\eta\hat{s}}.
\end{aligned}$$

The characteristic equation corresponding with the above matrix is given by

$$\gamma^3+Z_4\gamma^2+Z_5\gamma+Z_6=0,$$

where,

$$\begin{aligned}
Z_4&=-(b_{11}+b_{22}+b_{33}),\ Z_5=b_{22}b_{33}+b_{11}b_{33}+b_{11}b_{22}-b_{12}a_{21},\\
Z_6&=-\det(J_{\mathcal{E}}|\mathcal{E}_3)=-[b_{11}b_{22}b_{33}-b_{12}b_{21}b_{33}].
\end{aligned}$$

According to Routh-Hurwitz criterion, $\mathcal{E}_3$ is locally asymptotically stable iff $Z_4>0$, $Z_6>0$, and $Z_4Z_5-Z_6>0$.
Also, the Jacobian matrix $J_{\mathcal{E}}$ at the coexisting equilibrium point $\mathcal{E}^*(s^*,i^*,p^*)$ associated with model (5) is given as:

$$J(\mathcal{E}^*)=\begin{bmatrix}c_{11}&c_{12}&c_{13}\\c_{21}&c_{22}&c_{23}\\c_{31}&c_{32}&c_{33}\end{bmatrix},$$

where,

$$\begin{aligned}
c_{11}&=-\frac{rs^*}{1+\gamma i^*}+\frac{\alpha(1-\vartheta)^2s^*i^*}{(a+(1-\vartheta)s^*)^2}+\frac{\eta\beta s^*p^*}{(1+\eta s^*)^2(1+\mu p^*)},\\
c_{12}&=-s^*\left[\frac{r(2-s^*)}{(1+\gamma i^*)^2}+\frac{\alpha(1-\vartheta)}{a+(1-\vartheta)\bar{s}}\right],
\end{aligned}$$

$$c_{13} = -\frac{\beta s^*}{(1+\eta s^*)(1+\mu p^*)^2}, \quad c_{21} = \frac{\alpha a(1-\vartheta)i^*}{(a+(1-\vartheta)s^*)^2},$$
$$c_{22} = \frac{\eta b i^* p^*}{(1+\eta i^*)^2(1+\mu p^*)}, \quad c_{23} = -\frac{bi^*}{(1+\eta i^*)(1+\mu p^*)^2},$$
$$c_{31} = \frac{\beta c p^*}{(1+\eta s^*)^2(1+\mu p^*)}, \quad c_{32} = \frac{bcp^*}{(1+\eta i^*)^2(1+\mu p^*)},$$
$$c_{33} = -\frac{\mu b c i^* p^*}{(1+\eta i^*)(1+\mu p^*)^2} - \frac{\mu\beta c s^* p^*}{(1+\eta s^*)(1+\mu p^*)^2}.$$

The characteristic equation associated with the above matrix is

$$\psi^3 + Z_7\psi^2 + Z_8\psi + Z_9 = 0,$$

where,

$$Z_7 = -(c_{11}+c_{22}+c_{33}),$$
$$Z_8 = -(c_{12}c_{21}+c_{13}c_{31}+c_{23}c_{32}-c_{11}c_{22}-c_{11}c_{33}-c_{22}c_{33}),$$
$$Z_9 = -(c_{11}c_{22}c_{33}+c_{12}c_{23}c_{31}+c_{13}c_{21}c_{32}-c_{13}c_{31}c_{22}-c_{12}c_{21}c_{33} - c_{11}c_{23}c_{32}).$$

If $Z_7 > 0, Z_9 > 0$, along with the condition $Z_7Z_8 - Z_9 > 0$, then model (5) is locally asymptotically stable around the coexisting equilibrium point $\mathcal{E}^*(s^*, i^*, p^*)$.

A.2.

Proof. The global stability of the model (5) around the endemic equilibrium $\mathcal{E}^*(s^*, i^*, p^*)$. A function of Lyapunov form

$$L(s,i,p) = s - s^* - s^* ln\frac{s}{s^*}) + (i - i^* - i^* ln\frac{i}{i^*}) + (p - p^* - p^* ln\frac{p}{p^*}.$$

Here, $L(s,i,p) \geq 0$ since $\psi - 1 \geq ln\,\psi$ for $\psi > 0$ and $L(s^*,i^*,p^*) = 0$. Differentiating L with respect to t, we obtain

$$\frac{dL}{dt} = \left(\frac{s-s^*}{s}\right)\frac{ds}{dt} + \left(\frac{i-i^*}{i}\right)\frac{di}{dt} + \left(\frac{p-p^*}{p}\right)\frac{dp}{dt},$$
$$= (s-s^*)\left\{-\frac{r(s+i)}{1+\gamma i} - \frac{\alpha(1-\vartheta)i}{a+(1-\vartheta)s} - \frac{\beta p}{(1+\eta s)(1+\mu p)} + \frac{r(s^*+i^*)}{1+\gamma i^*} + \frac{\alpha(1-\vartheta)i^*}{a+(1-\vartheta)s^*} + \frac{\beta p^*}{(1+\eta s^*)(1+\mu p^*)}\right\} + (i-i^*)\left\{\frac{\alpha(1-\vartheta)s}{a+(1-\vartheta)s} - \frac{bp}{(1+\eta i)(1+\mu p)} - \frac{\alpha(1-\vartheta)s^*}{a+(1-\vartheta)s^*} + \frac{bp^*}{(1+\eta i^*)(1+\mu p^*)}\right\} + (p-p^*)\left\{\frac{cbi}{(1+\eta i)(1+\mu p)} + \frac{c\beta s}{(1+\eta s)(1+\mu p)} - \frac{cbi^*}{(1+\eta i^*)(1+\mu p^*)} - \frac{c\beta s^*}{(1+\eta s^*)(1+\mu p^*)}\right\}.$$

After some simplifications, we get

$$\frac{dL}{dt} = -(s-s^*)\left\{\left(\frac{s+i}{1+\gamma i} - \frac{s^*+i^*}{1+\gamma i^*}\right)r + \left(\frac{(1-\vartheta)i}{a+(1-\vartheta)s} - \frac{(1-\vartheta)i^*}{a+(1-\vartheta)s^*}\right)\alpha + \left(\frac{p}{(1+\eta s)(1+\mu p)} - \frac{p^*}{(1+\eta s^*)(1+\mu p^*)}\right)\beta\right\}$$
$$- (i-i^*)\left\{b\left(\frac{p}{(1+\eta i)(1+\mu p)} - \frac{p^*}{(1+\eta i^*)(1+\mu p^*)}\right)\right.$$
$$\left. - \alpha\left(\frac{(1-\vartheta)s}{a+(1-\vartheta)s} - \frac{(1-\vartheta)s^*}{a+(1-\vartheta)s^*}\right)\right\}$$
$$- (p-p^*)c\left\{b\left(\frac{\eta\,\mu\,(i^*p - i^*p^*) - \mu\,(ip^* - i^*p) - (i-i^*)}{(1+\eta i)(1+\mu p)(1+\eta i^*)(1+\mu p^*)}\right)\right\}$$
$$- (p-p^*)c\left\{\beta\left(\frac{\eta\,\mu\,(s^*p - s^*p^*) - \mu\,(sp^* - s^*p) - (s-s^*)}{(1+\eta s)\,(1+\mu p)\,(1+\eta s^*)\,(1+\mu p^*)}\right)\right\}.$$

Now, we see that $\frac{dL}{dt}$ is negative definite in the region: $G = \{(s,i,p) : s > s^*, i > i^* \text{ and } p > p^*)\ or\ s < s^*, i < i^*\ and\ p < p^*\}$ and consequently, for all solutions in G, L is a Lyapunov function. □

A.3.

Proof. If $h_1 = h_1^{TC} = r$, then $\det(J_{\mathcal{E}}|\mathcal{E}_0) = 0$ and hence the Jacobian matrix $J_{\mathcal{E}}|_{h_1=h_1^{TC}}$ (at $\mathcal{E}_0$) and $J_{\mathcal{E}}^T|_{h_1=h_1^{TC}}$ (at $\mathcal{E}_0$) corresponding to zero eigenvalue, respectively then

$$S = \begin{bmatrix} s_1 \\ s_2 \\ s_3 \end{bmatrix} = \begin{bmatrix} 1 \\ 0 \\ 0 \end{bmatrix},$$
$$I = \begin{bmatrix} i_1 \\ i_2 \\ i_3 \end{bmatrix} = \begin{bmatrix} 1 \\ 0 \\ 0 \end{bmatrix}.$$

Further, using Sotomayor's Theorem, we have

$$F_{h_1}(\mathcal{E}_0; h_1^{TC}) = \begin{bmatrix} 0 \\ 0 \\ 0 \end{bmatrix},$$
$$DF_{h_1}(\mathcal{E}_0; h_1^{TC})X = \begin{bmatrix} -1 & 0 & 0 \\ 0 & 0 & 0 \\ 0 & 0 & 0 \end{bmatrix}\begin{bmatrix} s_1 \\ s_2 \\ s_3 \end{bmatrix} = \begin{bmatrix} -1 \\ 0 \\ 0 \end{bmatrix}.$$

Thus,

$$\triangle_1 = Y^T F_{h_1}(\mathcal{E}_0; h_1^{TC}) = 0,$$
$$\triangle_2 = Y^T[DF_{h_1}(\mathcal{E}_0; h_1^{TC})X] = -1 \neq 0,$$
$$\triangle_3 = Y^T[D^2F_{h_1}(\mathcal{E}_0; h_1^{TC})(X,X)],$$
$$= i_1(f_{ss}s_1^2 + f_{ii}s_2^2 + f_{pp}s_3^2 + 2f_{si}s_1s_2 + 2f_{ip}s_2s_3 + 2f_{ps}s_1s_3) + i_2(g_{ss}s_1^2 + g_{ii}s_2^2 + g_{pp}s_3^2 + 2g_{si}s_1s_2 + 2g_{ip}s_2s_3 + 2g_{ps}s_1s_3) + i_3(h_{ss}s_1^2 + h_{ii}s_2^2 + h_{pp}s_3^2 + 2h_{si}s_1s_2 + 2h_{ip}s_2s_3 + 2h_{ps}s_1s_3),$$
$$= -2r \neq 0,$$

where

$$f(s,i,p) = \frac{rs(1-s-i)}{1+\gamma i} - \frac{\alpha(1-\vartheta)si}{a+(1-\vartheta)s} - \frac{\beta sp}{(1+\eta s)(1+\mu p)} - h_1 s,$$
$$g(s,i,p) = \frac{\alpha(1-\vartheta)si}{a+(1-\vartheta)s} - di - \frac{bip}{(1+\eta i)(1+\mu p)} - h_2 i,$$
$$h(s,i,p) = -\delta p + \frac{cbip}{(1+\eta i)(1+\mu p)} + \frac{c\beta sp}{(1+\eta s)(1+\mu p)}.$$

Hence, by Sotomayor's Theorem, model (5) undergoes a transcritical bifurcation around $\mathcal{E}_0$. □